www.czasopisma.pan.pl PAN www.journals.pan.pl

ARCHIVES of FOUNDRY ENGINEERING

ISSN (2299-2944)
Volume 2023
Issue 2/2023

72 – 79

10.24425/afe.2023.144298

11/2

Published quarterly as the organ of the Foundry Commission of the Polish Academy of Sciences

Identification of the Parameters of the Model Generating the Microstructure in the Integrated Heating-Remelting-Cooling Process

P. Marynowski *, M. Hojny, T. Dębiński, D. Cedzidło
AGH University of Science and Technology, Poland
* Corresponding author. E-mail address: pmarynow@agh.edu.pl

Received 03.08.2022; accepted in revised form 22.02.2023; available online 26.05.2023

Abstract

This paper identifies and describes the parameters of a numerical model generating the microstructure in the integrated heating-remelting-cooling process of steel specimens. The numerical model allows the heating-remelting-cooling process to be simulated comprehensively. The model is based on the Monte Carlo (MC) method and the finite element method (FEM), and works within the entire volume of the steel sample, contrary to previous studies, in which calculations were carried out for selected, relatively small areas. Experimental studies constituting the basis for the identification and description of model parameters such as: probability function, initial number of orientations, number of cells and number of MC steps were carried out using the Gleeble 3800 thermo-mechanical simulator. The use of GPU capabilities improved the performance of the numerical model and significantly reduced the simulation time. Thanks to the significant acceleration of simulation times, it became possible to comprehensively implement a numerical model of the heating-transformation-cooling process in the entire volume of the test sample. The paper is supplemented by results of performance tests of the numerical model and results of simulation tests.

Keywords: Heating-Remelting-Cooling process, Gleeble 3800, Monte Carlo method, Grains

1. Introduction

Prediction of the parameters of the structure subjected to heat treatment, such as recrystallization kinetics or grain size, is necessary to optimize the process conditions and properties of the final product. The micro model of the grain growth is based on the Monte Carlo (MC) method and minimizing the energy of the system [1, 2]. Physical simulations of the heating-remelting-cooling process were carried out on the thermo-mechanical simulator, Gleeble 3800 series.

Experimental studies constituted the basis for the identification and description of model parameters such as: probability function, initial number of orientations, number of cells and number of MC steps. The probability function, B_m, influences the probability of changing the value of a cell in the whole space of MC. If the function B_m takes a value of 0, then the probability of changing the value of the cell takes a value of 0. The greater the value of the probability function for a given temperature, the higher the probability of changing the value of the cell. Controlling the range of the exponent, n, of the B_m function allows the grain distribution to be changed, which influences controlling the ranges of the

sample zones. Increasing the exponent shifts the zone ranges (ignoring the remelting zone) towards the center of the sample. The influence of the exponent on the simulation decreases as the exponent value increases. If the value of the exponent is 0, the probability function takes a constant value of 1, which causes the number of grains to be constant in the whole sample (ignoring the melting zone). The number of MC steps has an impact on the number of grains. The number of grains decreases as the number of MC steps increases. The number of cells in the MC space influences the change in the number of grains. As the number of cells increases, the number of grains in the sample increases as well. The number of orientations has an impact on the number of grains. As the number of orientations increases, the number of grains increases as well. Our model is distinguished by including the remelting process (the formation of the liquid and solid phase mixture), and the impact of the temperature distribution and gradient, which is diversified in the whole sample volume, on the grain growth dynamics. This effect has been achieved by applying a special boundary probability function, which takes into account the change in probability depending on the temperature. This approach allowed us to include the whole volume of the sample and estimate the grain size in each sample zone. In the center of the sample the highest dynamics of the temperature changes are achieved. The probability function changes from a value of 1 to 0 (to the areas with a lower temperature). The kinetics of the grain growth is simulated by a random selection of cells from all possible cells, and an attempt to change their states by replacing a specific parameter describing their affinity to a specific grain orientation with a parameter of the neighboring grain. Cells located within a grain that do not have a neighborhood belonging to a different grain type, cannot change their state. When the chosen cell is subjected to an attempt at state change, a random choice is made from of one state from all the neighboring states and assigned to it.

The MC method [3 - 6] was introduced into general use in the 1940s by scientists working on the development of nuclear weapons at the Los Alamos Institute. The method was used to simulate the random behavior of neutrons in fissionable materials. As computer processing power developed, it has begun to be used to simulate many physical and mathematical issues. The name MC does not designate a single specific computational method, but a whole class of similar methods, the basic assumptions of which are based on a single algorithm [7, 8]. Due to its advantages, the MC method is widely used in the simulation of many different physical processes. There is a lot of information in the literature describing the application of the MC method in the process of solidification [9 - 11] and welding [12 - 16]. Due to the presented ways of using the MC method, it can be concluded that this method allows a comprehensive simulation of the heating-remelting-cooling process and the phenomena occurring during this process to be carried out [2]. The main disadvantage of the MC method is the very long calculation time. For the sake of the accuracy and correctness of the MC method, a random number generator is used. The MC time steps are not typical time steps, therefore, it is difficult to determine the actual calculation time in the MC method.

To compensate for the significant calculation time, GPU capabilities were used. Currently, more and more simulation programs are taking advantage of GPU's capabilities thanks to the continued development of graphics cards. The GPU allows complex calculations to be performed in much less time than on a CPU. One of the requirements is to properly parallelize the algorithm so that calculations are performed on multiple threads. With the use of GPU technology, it becomes possible to obtain results in a much shorter time, making it possible to repeatedly test the implemented algorithm. In order to use the GPU, the CUDA architecture is used, which is based on C and C++ language. The CUDA architecture has extensive documentation, its own libraries and, most importantly, is developed and supported [17]. Currently, there are many solutions using the GPU to accelerate simulations previously performed with a CPU only. The paper [18] describes the use of GPU to enhance the performance of a simulation using the MC method for chemotherapy dosing. In [19], differences in the CPU and GPU performances in calculating particle trajectories under static and dynamic force fields were presented. It was found there that the calculation of a large number of particle trajectories was about 356 times faster than in a CPU-only solution. In general, the use of GPUs usually allows calculations for ion deployment simulations to be 10 to 100 times faster than in CPU-based solutions [20 - 23].

The main goals of the study are the identification and description of the parameters of a numerical model generating a microstructure as similar to the experimental as possible, in the integrated heating-remelting-cooling process of steel specimens, and the transfer from a CPU-based model to a GPU-based one.

2. Numerical model

Details of the numerical model that generates a digital representation of the microstructure are presented in the papers [1 - 2].

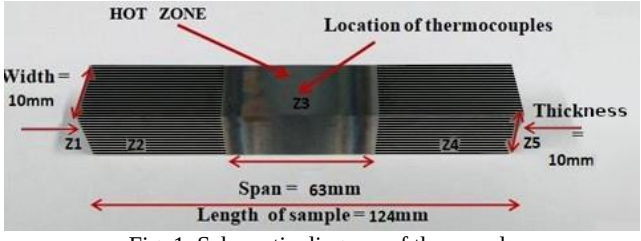

Fig. 1. Schematic diagram of the sample

Fig. 1 shows a schematic diagram of the location of five heat exchange zones. These locations are marked from Z1 to Z5. Z2 and Z4 define the contact area between the sample and the copper grips, where intense heat dissipation into the tool occurs. Zones Z1, Z3, and Z5 define the areas of the sample where there is free heat exchange with the environment. A flow of electric current through a conductor is always accompanied by a release of heat. This means that in elements with a certain resistance, the electrical energy is converted into heat energy.

The macro-scale numerical model is based on the solution of the Fourier-Kirchhoff differential equation, with an internal heat source. The micro-model of grain growth is based on the MC method. The MC method is a probabilistic method and is based on minimizing the energy of the system.

The micro model is characterized by including the remelting process (formation of the liquid-solid phase) and the effect of the

temperature gradient that forms in the volume of the element on the dynamics of grain growth in the simulation. This effect is achieved by using a special boundary mobility function that takes into account the temperature-dependent probability change, $B_m(T)$. This approach allowed the sample volume to be included comprehensively in numerical simulations, and the grain size to be estimated in each of the sample zones. The central (middle) region of the sample shows the greatest dynamics of temperature change. In this area, the maximum temperature values are reached ($B_m(T) = 1$) and they decrease towards the areas where the temperature, as a result of intensive cooling, reaches much lower values ($B_m(T) = 0$). The kinetics of grain growth is simulated by randomly selecting cells and attempting to change their states by changing the Q describing the orientation of a grain to a neighboring grain. Cells belonging to a grain, which does not have a neighbor belonging to another grain, cannot change their state. When a selected cell is subjected to a state change, a random change to the state of any of its neighbors is generated.

The simulation of the heating-remelting-cooling process proceeds as follows: when the temperature of a given cell is equal to or greater than the assumed melting temperature, melting is simulated by randomly assigning a state to the cell, different than the states of its neighbors' cells. The grain degradation and growth result in an increase in energy. The grain algorithm applied in the solidification process randomly selects the state out of the neighboring cell states, reduces the energy, and forms a new grain of at least two neighboring cells.

The multi-scale model of the heating-remelting-cooling process presented in [1 - 2] is an innovative and original approach to the simulation of the first stage preceding the deformation in the semi-solid state, i.e. heating a sample to a set nominal test temperature. Its numerical implementation was included in the original DEFFEM3D [1 - 2] software. Its main purpose is to effectively support physical simulations performed with Gleeble 3800 simulators by limiting, among others, the number of costly experimental tests. The integrated DEFFEM3D software proposed the use of a multi-scale model involving thermal calculations at the macro scale using the finite element method. Calculations related to modeling the grain growth dynamics were carried out on the micro scale using the MC method.

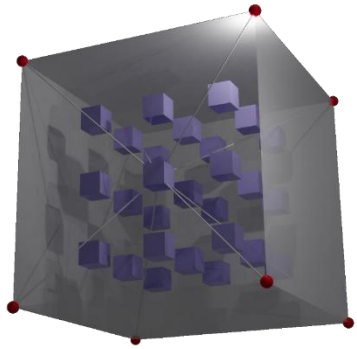

Fig. 2. Sample image showing how the temperature is interpolated from a FEM to an MC cell

The temperature field is calculated using the finite element method (FEM), and then the temperature values are interpolated using a shape function to each cell of the MC space.

The numerical model applied was subjected to the identification and verification of the parameters that have a decisive influence on the course of the simulation. For this purpose, an experiment was performed.

3. Experiment

Physical simulations of the heating-remelting-cooling process were carried out on a thermo-mechanical simulator of the Gleeble 3800 series, presented in [2]. The tested material was steel S355 with its chemical composition shown in Tab. 1.

Table 1.
Chemical composition of steel S355, %

C	Mn	Si	P	S	Cr	Ni
0.16	1.26	0.26	0.011	0.009	0.14	0.06

The tests used rectangular-shaped specimens with dimensions of 10x10x124 mm. In addition, the use of a quartz shield to protect the interior of the simulator from liquid metal was abandoned to avoid disturbances affecting the heat transfer mechanism. The first step was to heat the sample to 1400 ℃ at a constant heating rate of 5 ℃/s and then to 1440 ℃ at a rate of 1 ℃/s. The next step was controlled cooling at a rate of 10 ℃/s to a temperature of 800 ℃. The final stage of the experiment was the free cooling of the sample in the Gleeble 3800 simulator tool system to the ambient temperature. During the experiment, the temperature was recorded. In addition, the current intensity was recorded. Fig. 3 shows an actual preview of the experiment.

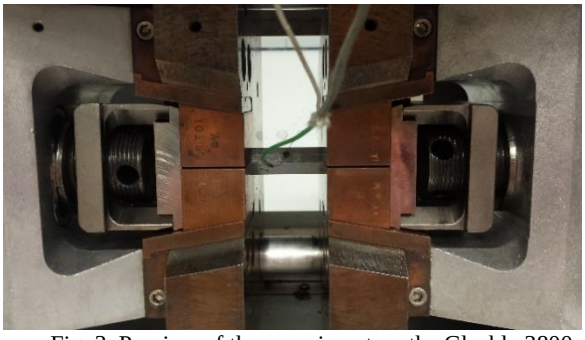

Fig. 3. Preview of the experiment on the Gleeble 3800 simulator

Microstructure studies were carried out on selected longitudinal sections in the axis of the sample, counting from the center of the heating zone marked as 0 mm, at a distance of 5, 10, 15, 20, 25, and 30 mm, respectively. The analysis of the obtained microstructure images shows the existence of differentiated zones, with different densities (sizes) of cells. The coarse-grained structure was revealed at the sample center and at a distance of 5 mm from it (coarse-grained structure). Moving towards the copper grips (decreasing temperature) at distances of 10, 15 and 20 mm from the sample center, the structure becomes more fine-grained with a fading visible grain boundary. At a distance of 25 mm from the center of the sample, the resulting structure is practically the same as the initial structure.

4. Simulation

The simulations were conducted for the selected sample volume, due to the existence of symmetry planes. The simulation range was limited to a distance of 40 mm from the center of the sample. At large distances from the center of the sample, where the temperature does not exceed T_0, there are no changes from the initial random state of the cells. For the simulations two ranges were used:

- A - with a volume of 40 mm x 10 mm x 10 mm, using 20 x 5 x 5 = 500 elements
- B - with a volume of 40 mm x 2 mm x 2 mm, using 20 x 1x 1 = 20 elements

Each element is the same, with a size of 2 mm x 2 mm x 2 mm. The same results were observed when comparing the microstructures in the longitudinal section of the sample for Ranges A and B. Range A was used to calculate and simulate the exponent of the probability function and the number of the MC steps. Range B was used to calculate the number of cells and the orientations of cells in the MC space. Range B allows a higher cell density to be studied in the simulation. The number of elements is crucial for the simulation time, the higher the number of elements, the longer the simulation time. For the simulation, we decided to use both ranges.

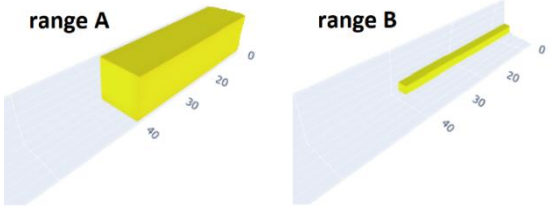

Fig. 4. Range A and B

Table 2.
Sample simulation times (CPU-based) for different number of elements

Number of elements	Time, *s*
1	452
20	604
500	4827

Table 3.
Information about all parameters, which were used in the simulations

Type of simulation	Simulation parameters			
	n	*p*	*c*	*o*
Exponent of probability function, *n*	0, 10, 12, 32	100	100	54
Number of MC steps, *p*	12	1, 10, 100	100	54
Number of MC cells, *c*	12	100	50, 200, 350	54
Number of cell orientation, *o*	12	100	100	3, 54, 104

4.1. Exponent of the mobility/probability function

Increasing the exponent *n* shifts the zone ranges (ignoring the melting zone) toward the center of the simulation. The impact of changing the exponent decreases as the exponent increases. For the parameter $n = 0$, the mobility function takes a constant $value = 1$, making the number of grains constant throughout the sample (ignoring the remelting zone). Fig. 5 shows the calculated microstructure of the sample for *n* equal to 0, 10, 12 and 32, which illustrate the shift of zone ranges within the sample as the value of n changes. For $n = 0$, a coarse-grained microstructure was obtained throughout the longitudinal section of the sample.

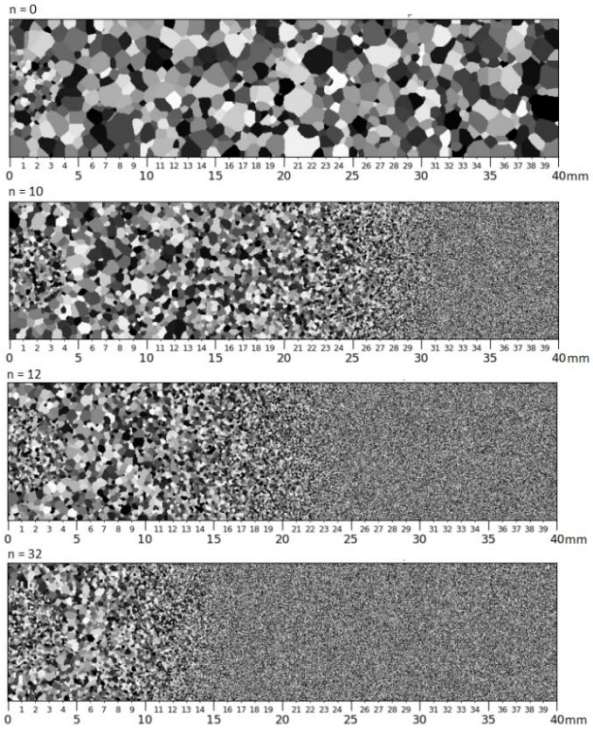

Fig. 5. Longitudinal sections for different values of the exponent, *n*

4.2. The number of steps in the MC method

As the number of steps p increases, the number of grains becomes smaller. Fig. 6 shows the calculated microstructure for the number of steps $p = 1.10\ and\ 100$. From the longitudinal sections of the sample shown, it is clear that the number of grains decreases as the number of steps p increases. For $p = 1$, a fine-grained microstructure was obtained, and for $p = 100$ the macrostructure obtained was coarse-grained.

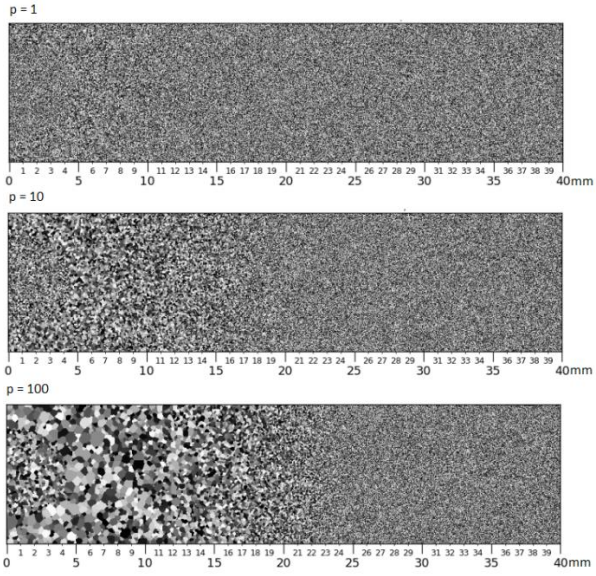

Fig. 6. Longitudinal sections for different values of the number of steps, *p*

4.3. The number of cells in the MC method

The calculated macrostructures for the number of cells $c = 50, 200\ and\ 350$ are shown in Fig. 9. From the cross sections shown, it is apparent that increasing the number of cells has an effect on increasing the number of grains in the sample. For $c = 50$, a coarse-grained microstructure was obtained, and for $c = 350$ – a fine-grained one.

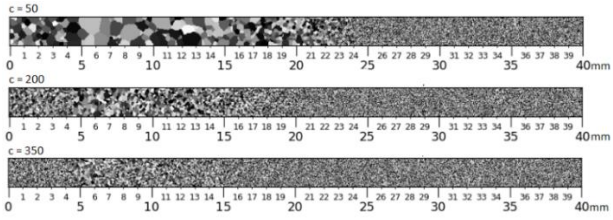

Fig. 7. Longitudinal sections for different values of the number of cells, *c*

4.4. The number of orientations in the MC method

As the number of orientations increases, the number of grains increases. The effect of the number of orientations on the number of grains decreases with the higher values of the number of orientations. Fig. 8 shows the microstructures on the longitudinal cross-section of the simulated sample for orientations $o = 3, 54, 104$. We can see an increase in the number of grains in the cross-section and a change in the number of orientations. As can be seen from the cross sections shown, the number of grains increases as the number of orientations increases.

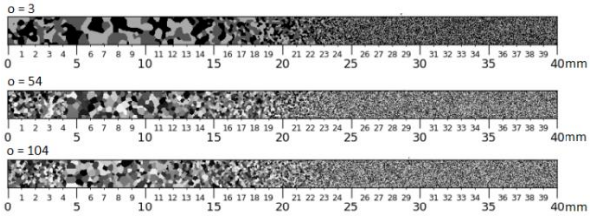

Fig. 8. Longitudinal sections for different values of the number of orientations, *o*

5. Identification of model parameters - experimental verification

The applied numerical model of the simulation of heating-remelting-cooling process was subjected to experimental verification. The main objective of the verification was to appropriately select the parameters of the simulation so that it reproduced the actual conditions of the process as accurately as possible. The obtained results in the form of images of microstructures were further analyzed.

The Saltykov Rectangle method [24] was used to calculate the number of grains in the mm^2 in images of microstructures from the experiment. According to this method, the number of grains in a square section is counted. The number of grains in the studied cross-section was taken as a sum:

$$n = n_{inside} + \frac{n_{intercepted}}{2} + 1 \tag{1}$$

where:

- n_{inside}- number of grains inside the cross section
- $\frac{n_{intercepted}}{2}$ – half of the number of grains passing through the edge of the section, not including the grains passing through the vertex
- 1 – the assumed number of grains passing through the vertices of the section

Using the above method, the number of grains in the cross-sections of the experimental sample was counted based on the images of the microstructure examined at distances of 0, 5, 10 and 15 mm. For distances of 20, 25, and 30 mm, the study was not carried out due to the size of the grains, as these grains were too small to be counted manually. The results of the grain counts are presented in Tab. 4.

Table 4.
The number of grains in the cross section of the experimental sample

Distance, mm	n_{inside}	$n_{intercepted}$	n
0	16	12	23
5	10	9	15.5
10	23	20	34
15	118	43	140.5

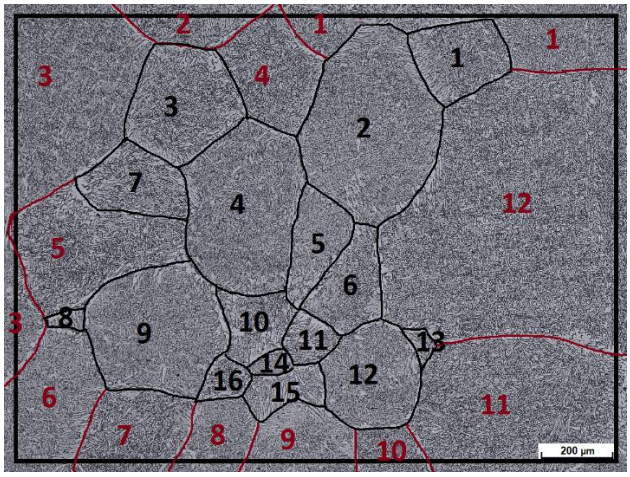

Fig. 9. Sample using the Saltykov Rectangle method

Fig. 9 shows a sample using the Saltykov Rectangle method. All grains were selected by the manual method only. 16 grains are inside the cross section and 12 pass through the edge of the section.

The parameters of the numerical model were identified by comparing the number of grains at distances of 0, 5, 10, and 15 mm from the center of the sample. Based on the study, the parameters were identified showing the agreement between the experimental results and the simulation. The following magnitudes of the examined parameters were assumed:

- Exponent of the mobility function: $n = 24$
- Number of steps of the MC method: $p = 100$
- Number of MC cells: $c = 100$
- Number of MC orientations: $o = 54$

Tab. 5 presents a comparison of the number of grains obtained by the experiment and by the simulation. The absolute and relative error values were also determined.

Table 5.
The number of grains in the cross section of the sample (experiment and simulation)

Distance, mm	Number of the grains		Error	
	exp.	sim.	absolute, mm	relative, %
0	23	22.7	0.3	1.3
5	15,5	13.9	1.6	10.3
10	34	30.3	3.7	10.8
15	140,5	135.2	5.3	3.7

Based on the results of the number of grains and the relative error values, it can be concluded that the accuracy is at a very high level. Error values of 10% were obtained for distances of 5 and 10 mm. For distances of 0 and 15 mm, these values were 1.3% and 3.7%, respectively.

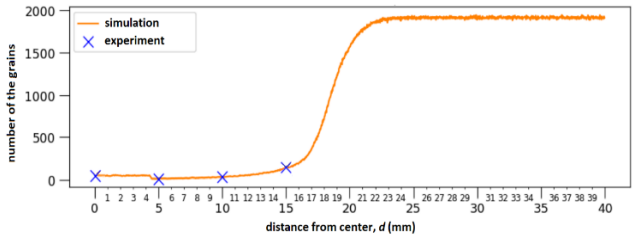

Fig. 10. Dependence of the grain number on distance for simulation and selected parameters and experiment

Fig. 10 shows a curve of the dependence of the number of grains on distance for experimental data and for the simulation with the assumed parameters of the process simulation. It can be seen here that there is a very high convergence of results, which allows us to find that the selection of the parameters of the simulation process and its further use were correct. Fig. 11 presents a comparison of the longitudinal cross sections of the samples obtained by the simulation and experiment.

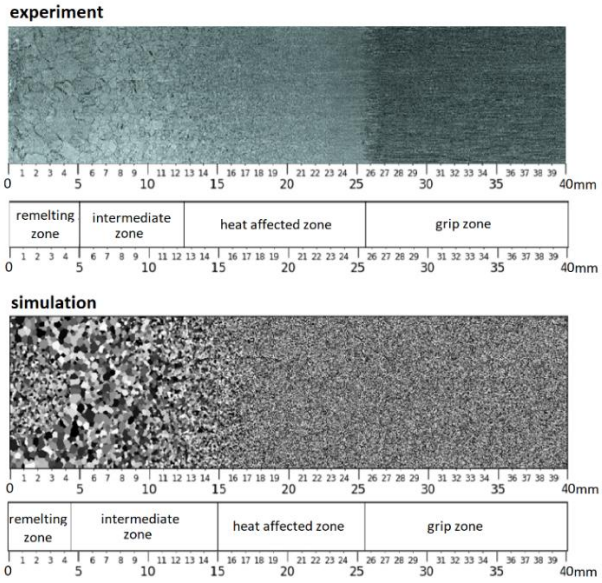

Fig. 11. Range of zones on longitudinal sections of the samples: simulation and experiment

Proprietary software was applied for determining the zones. Due to the complexity of the operation, an evaluation was performed to select the filter binarization levels for extracting the remelting zone, intermediate, heat affected and grip zones. Microscopic images are characterized by the presence of fine grains with varying levels of brightness of structural elements, it was decided to reduce the number of image details and filter out the so-called noise. Further image processing made it possible to extract the recognized areas and to obtain an image of zones with a continuous, uniform distribution of shades of gray, and with a degree of brightness different from the neighboring zones. Operations were performed in the following steps: median filter, morphological closure filter and, finally, contrast stretching. For such a filtering methodology, an image with highlighted zone areas

and a significant reduction in noise was obtained. As a result, the parameters defining individual areas, along the cross-section of the sample, were obtained on the basis of a histogram of brightness changes along the studied vector. Finally, the individual zones can be determined.
Fig. 12 shows the distribution of cells whose initial orientation is different from the final one (yellow).

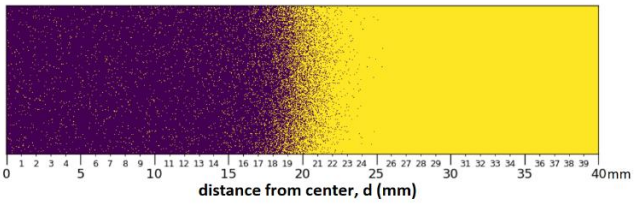

Fig. 12. Longitudinal cross-section of a sample in which the final orientation is different than the initial one

6. GPU-based simulations

The second goal of the study was to implement the CPU-based program to the GPU-based one and to compare both of them. The use of GPU capabilities improves the performance of the numerical model and significantly reduces the simulation time. A computer with a graphic card GeForce GTX 750 Ti with 2 GB RAM and processor i3 6th 2.8 GHz was used for the simulations. Tab. 6 shows a comparison of the result simulation time for the CPU-based and GPU-based implemented model. The model parameters were the same in both models: exponent of probability function, $n = 24$; number of MC steps, $p = 100$; number of MC cells, $c = 100$; and number of cell orientations, $o = 54$.

Table 6.
Simulations time on CPU-based and GPU-based model

	Architecture	
	CPU-based	GPU-based
Time of simulation, *s*	1219.38	23.47

For comparison, simulation times between GPU and CPU showed a more than 52-fold acceleration in favor of the GPU.

7. Discussion of results

Analyzing the microstructures of the test specimen on the longitudinal section, four main zones are visible (Fig. 11**):**

Table 7.
Distance from center for four zones

Zone	Experiment	Simulation
Remelting zone	0-5 mm	0-4.5 mm
Intermediate zone	5-12.5 mm	4.5-15 mm
Heat-affected zone	12.5-25.5 mm	15-25.5 mm
Grip zone	25.5-40 mm	25.5-40 mm

- remelting zone: where local remelting of the sample takes place followed by the growth of new grains, depending on the local cooling rates achieved,
- intermediate zone: where local remelting does not occur, but it features a dynamic grain growth as a result of the high temperatures achieved in this area,
- heat-affected zone: characterized by low grain growth dynamics due to a much smaller range of temperatures reached,
- grip zone: characterized by negligible grain growth dynamics due to the low range of temperatures reached.

The intermediate zone is much longer in the simulation (7.5 mm) than in the experiment (10.5 mm). The heat-affected zone is shorter in the simulation (10.5 mm) than in the experiment (13 mm). These results depend on the model parameters. Future work on a new way to approximate those parameters can bring better results.

The positions of the zones presented in Fig. 11 show results that are very similar to each other. In Fig. 12, it can be seen that changes in the cell orientation occur from 0 to 25.5 mm from the sample center. This corresponds to the range from the remelting zone to the heat affected zone. This confirms that the selection of process parameters is consistent.

8. Conclusion

The most important aspect of the paper was the identification and description of the parameters of a complex numerical model of the heating-remelting-cooling process based on experimental data. Physical simulations of the heating-remelting-cooling process were carried out on the thermo-mechanical simulator, Gleeble 3800 series.

The obtained results made it possible to identify the parameters of the numerical model, which exists in the form of the author's DEFFEM3D software [1, 2]. Therefore, it is possible to effectively support physical simulations carried out using the Gleeble 3800 simulator by reducing the number of expensive experimental trials. It also enables additional information to be obtained, such as local cooling rates at any point in the volume of the sample tested. Correctly verified and identified parameters of the numerical model significantly improved the performance of simulations and allowed us to obtain very accurate results.

The second aspect was the use of GPU capabilities in improving the performance of the numerical model and significantly reducing simulation time. The numerical model was adjusted for the use of modern GPU technologies, so that calculation times were significantly accelerated. For comparison, simulation times between the GPU and CPU showed a more than 52-fold acceleration in favor of the GPU. Thanks to the significant acceleration of simulation times, it became possible to comprehensively implement a numerical model of the heating-transformation-cooling process through the entire volume of the test sample.

The optimized simulation system allows the grain growth model of heated samples to be computed, and allows additional information to be acquired such as local cooling rates at any point within the volume of the test sample. The compatibility of simulation results with the experimental data, combined with the

short execution time of the simulation, indicates that the software can be used in practice for microstructure studies.

Acknowledgment

The work was completed as a part of fundamental research financed by the Ministry of Science and Higher Education, grant no. 16.16.110.663.

References

[1] Hojny, M. (2018). *Modeling steel deformation in the semi-solid state*. Switzerland: Springer.
[2] Hojny, M., Głowacki, M., Bała, P., Bednarczyk, P. & Zalecki, W. (2019). A multiscale model of heating- remelting-cooling in the Gleeble 3800 thermo-mechanical simulator system., *Archives of Metallurgy and Materials.* 64(1), 401-412. DOI: 10.24425/amm.2019.126266.
[3] Tong, M., Li, D. & Li, Y. (2004). Modeling the austenite – ferrite diffusive transformation during continuous cooling on a mesoscale using Monte Carlo method. *Acta Materialia.* 52(5), 1155-1162. DOI:10.1016/j.actamat.2003.11.006.
[4] Tong, M., Li, D. & Li, Y. (2005). A q-state Potts model based Monte Carlo method used to model the isothermal austenite – ferrite transformation under non-equilibrium interface condition. *Acta Materialia.* 53(5), 1485-1497. DOI:10.1016/j.actamat.2004.12.002.
[5] Mathea, P. & Novak, E. (2007). Simple Monte Carlo and the metropolis algorithm. *Journal of Complexity.* 23, 673-696. DOI:10.1016/j.jco.2007.05.002.
[6] Saito, Y. & Enomoto, M., (1992). Monte carlo simulation of grain growth. *ISIL International.* 32(3), 267-274.
[7] Blikstein, P. & Tschipschin, A.P. (1996). Monte Carlo simulation of grain growth. *Materials Research*. 2(3), 133-137.
[8] Shonkwiler, R.W., Mendivil, F. (2009). *Explorations in Monte Carlo methods.* Springer.
[9] Gao, J. & Thompson, R.G. (1997). Monte Carlo simulation of solidification. *Superalloys*. 718, 625, 706, 77-86.
[10] Das, A. & Fan, Z. (2004). A Monte Carlo simulation of solidification structure formation under melt shearing. *Materials Science and Engineering.* 365(1-2), 330-335. DOI: 10.1016/j.msea.2003.09.043.
[11] Zhu, P., Smith R.W. (1992). A Monte Carlo simulation of microstructural evolution during solidification. *Modeling of Coarsening and Grain Growth*. 85-99.
[12] Rodgers, T., Mitchell, J. & Tikare, V. (2017). A Monte Carlo model for 3D grain evolution during welding. *Modelling and Simulation in Materials Science and Engineering.* 25(6), 064006. DOI: 10.1088/1361-651X/aa7f20.
[13] Schmidt, R. (1987). The Monte Carlo method in welding practice. *Welding International.* 1(10), 983-985. https://doi.org/10.1080/09507118709449049.
[14] Haire, K.R., Windle, A.H. (2001). Monte Carlo simulation of polymer welding. *Computational and Theoretical Computer Polymer Science.* 11(3), 167-250. https://doi.org/10.1016/S1089-3156(00)00011-8.
[15] Zhang, Z.Q., Wu, M., Grujicic, Z. & Wan, Y. (2016). Monte Carlo simulation of grain growth and welding zones in friction stir welding of AA6082-T6. *Journal of Materials Science.* 51(4), 1882-1895. DOI:10.1007/s10853-015-9495-x.
[16] Yang, Z., Sista, S., Elmer, J. W. & Debroy, T. (2000). Three-dimensional Monte Carlo simulation of grain growth during GTA welding of titanium. *Acta Materialia.* 48, 4813-4825.
[17] NVIDIA® CUDA™ Architecture - Introduction & Overview. Retrieved July 17, 2022, from *https://developer.download.nvidia.com/compute/cuda/docs/CUDA_Architecture_Overview.pdf.*
[18] Jia, X., Gu, X., Graves, Y.J., Folkerts, M. & Jiang, S.B. (2011). GPU-based fast Monte Carlo simulation for radiotherapy dose calculation. *Journal Physics in Medicine & Biology.* 56(22), 7017-7031. DOI: 10.1088/0031-9155/56/22/002.
[19] Patro, R., Dickerson, J.P., Bista, S., Gupta, S.K., Varshney, A. (2012). *Speeding up particle trajectory simulation sunder moving force fields using GPUs*. Retrieved July 17, 2022, from *https://www.cs.umd.edu/~varshney/papers/gpu_tweezers.pdf*.
[20] GPU *Acceleration of molecular modeling applications.* Retrieved July 17, 2022, from *https://www.ks.uiuc.edu/Research/gpu/*.
[21] VMD. *Visual molecular dynamics*. Retrieved July 17, 2022, from *https://www.ks.uiuc.edu/Research/vmd/*.
[22] Stone, J.E., Phillips, J.C, Freddolino, P.L., Hardy, D.J., Trabuco, L.G. & Schulten, K. (2007). Accelerating molecular modeling applications with graphics processors. *Journal of Computational Chemistry*. 28(16), 2618-2640. DOI 10.1002/jcc.20829.
[23] Voort, G.V. (2013). *Grain size measurement: the saltykov rectangle*. Retrieved July 17, 2022, from https://vacaero.com/information-resources/metallography-with-george-vandervoort/1286-grain-size-measurement-the-saltykov-rectangle.html.
[24] Saltykov, S. (1958). *Stereometric Metallography.* (2nd edn.). Metallurgizdat. New York.